Advances in Nano Research, *Vol. 13, No.5 (2022) 465-474*
https://doi.org/10.12989/anr.2022.13.5.465

Guided waves of porous FG nanoplates with four edges clamped

Jing-Lei Zhao, Gui-Lin She, Fei Wu, Shu-Jin Yuan, Ru-Qing Bai,
Hua-Yan Pu* and Shilong Wang and Jun Luo

College of Mechanical and Vehicle Engineering, Chongqing University, Chongqing 400044, China

(*Received October 22, 2021, Revised June 21, 2022, Accepted July 4, 2022*)

Abstract. Based on the nonlocal strain gradient (NSG) theory and considering the influence of moment of inertia, the governing equations of motion of porous functionally graded (FG) nanoplates with four edges clamped are established; The Galerkin method is applied to eliminate the spatial variables of the partial differential equation, and the partial differential governing equation is transformed into an ordinary differential equation with time variables. By satisfying the boundary conditions and solving the characteristic equation, the dispersion relations of the porous FG strain gradient nanoplates with four edges fixed are obtained. It is found that when the wave number is very small, the influences of nonlocal parameters and strain gradient parameters on the dispersion relation is very small. However, when the wave number is large, it has a great influence on the group velocity and phase velocity. The nonlocal parameter represents the effect of stiffness softening, and the strain gradient parameter represents the effect of stiffness strengthening. In addition, we also study the influence of power law index parameter and porosity on guided wave propagation.

Keywords: functionally graded material; guided wave; nanoplates; nonlocal strain gradient theory; porous nanomaterials

1. Introduction

Due to its excellent mechanical, thermal, magnetic and optical properties, micro or nano structures are widely used in automobile, aerospace, electrical information, ocean engineering and other fields (for example, She *et al*. 2021, Lu *et al*. 2021, Zhang *et al*. 2021, Malikan *et al*. 2021a, b, Civalek *et al.* 2020, Eltaher *et al*. 2018, Barretta *et al*. 2019a, b, Jalaei and Civalek 2019, Ebrahimi and Barati 2017, 2016, Numanoğlu *et al*. 2022, Akgöz and Civalek 2013, 2014a, b, Zemri *et al*. 2015, Alazwari *et al*. 2022a, b, Ghandourah *et al*. 2021, Khadir *et al*. 2021, Bouhadra *et al*. 2021, Matouk *et al*. 2020, Singh and Azam 2021, Eltaher and Abdelrahman 2020). However, in practical applications, nanostructures are often subjected to various loads, resulting in wave propagation and other phenomena. As wave propagation is closely related to the working performance and fatigue failure of structures, it is necessary to analyze and evaluate the wave propagation and jump buckling of nanostructures, so as to provide a reliable theoretical basis for the design, development and application of nanostructures.

The wave propagation of nanostructures can be classified into guided wave and bulk wave. The body wave is considered that the body wave propagates freely in the matter, guided waves are different, they are affected by the boundary. The existing wave propagation analysis of nanostructures is mostly limited to the simple mechanical model of wave free propagation in matter, ignoring the influence of boundary conditions on the problem. Due to the various boundary conditions encountered in the process of wave propagation, the artificial assumption that the wave propagates freely in matter often leads to errors or even wrong results. Because guided wave can detect the local corrosion of the structure and have important engineering applications, it has attracted much attention. Therefore, the study of guided waves is expected to more accurately understand the propagation mechanism of elastic waves in nanostructures, which can effectively guide the optimal design and manufacturing of nanostructures.

The wave propagation of nanobeam, nanoplate, nanoshell and other nanostructures is a research hotspot in recent years. For example, Lim *et al*. (2015) proposed a new high-order nonlocal strain gradient (NSG) theory to predict the propagation mechanism of waves in nanobeams, which can simultaneously include the stiffness strengthening and softening effects. Based on the NSG theory, Liu and Lv (2018) studied the influence of material uncertainty on elastic waves in intelligent magneto electro elastic nanobeams. Wang and Liang (2019) studied the influence of various pore distributions on flexural waves in nanobeams. Ma *et al.* (2017) dicussed the propagation of waves in magneto electro elastic nanobeams. Zhou (2019) studied the impact of surface effect upon the propagations and topological properties of bending wave in periodic nanobeams. Ma *et al.* (2018a) examined the propagation characteristics of waves in piezoelectric nanoplates based on the nonlocal theory. Wang *et al.* (2019), Ma *et al.* (2018b) studied the propagation characteristics of elastic waves in functionally graded (FG) nanoshell.

In general, some achievements have been made in the research of body waves in nanostructures, which will lay a theoretical foundation for the application of nanostructures

*Corresponding author, Professor,
E-mail: phygood_2001@shu.edu.cn

ISSN: 2287-237X (Print), 2287-2388 (Online)

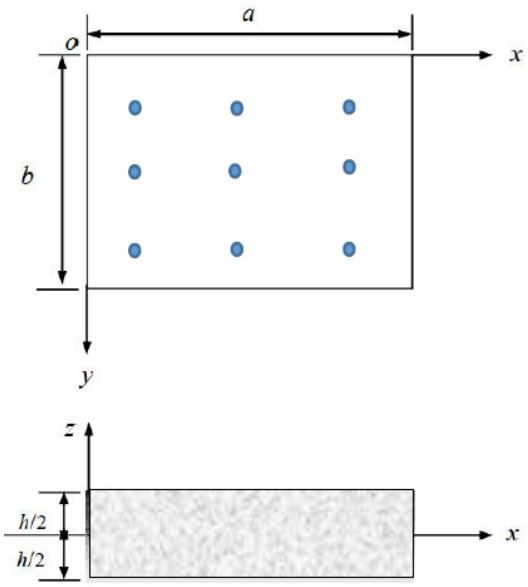

Fig. 1 A porous FG nanoplate

in engineering, but the existing research still has some limitations. When studying the wave propagation mechanism in nanostructures, many scholars assume that the wave response will be far away from the boundary conditions of nanostructures, and ignore the influence of boundary conditions on the wave propagation mechanism. Due to the lack of research on guided waves, Karami *et al*. (2018) first studied guided waves in a nano plate with four edges clamped. Compared with the solution process of bulk waves, the displacement function of guided waves is different and the computational complexity is larger. However, they (Karami *et al*. 2018) only studied the bending wave in the nanoplates, and the propagation characteristics of the expansion wave were ignored by them, and moreover, they only use the nonlocal theory, stiffness enhancement effect was also ignored by them.

Through literature search, we can find that, the research on guided waves in NSG porous FG nanoplates has not been reported. Therefore, at present, the guided waves in nanostructures have not been well understood and needs to be further studied. Thus, it is important to use the NSG theory to analyze the guided wave in the porous FG nanoplates, and the present paper is to solve this complex problem.

2. Nonlocal strain gradient for porous FG nanoplate

Consider an FG nanoplate as shown in Fig. 1. The four edges of the FG nanoplate are assumed to be clamped, the length, width and height of the plate are *a*, *b* and *h* respectively, there are many kinds of material models for functionally graded (FG) materials, for example, the classical material model is the *P* model, which is the classical power function form. However, scholars have found that the classical *P* model will also have some deviations in the evaluation of materials, because there will be pores in the manufacturing process of FG materials, which will undoubtedly affect the elastic modulus, density and Poisson's ratio of functionally graded materials (She *et al*. 2022, She 2021, Zhang and She 2022, Ding and She 2021). Therefore, it is necessary to consider the influence of pores on FG materials. Therefore, scholars proposed a modified *P* model to describe the elastic modulus, density and Poisson's ratio of FG materials, and found that this modified model is more accurate for the description of materials. Therefore, in the following analysis, we also use the modified material model to calculate the elastic modulus, density and Poisson's ratio of FG materials. And, the FG nanoplates are made from metal and ceramic, the equivalent mass density ρ, Poisson's ratio ν, elastic modulus E, and can be expressed as the function of the porosity volume fraction p and power law index N, as

$$P_f(z) = P_m + \left(\frac{z}{h} + \frac{1}{2}\right)^N (P_c - P_m) - \frac{p}{2}(P_c + P_m) \tag{1}$$

In Eq. (1), the subscript m and c denote the mental and ceramic, respectively. There are many theories for deriving the dynamic equations of plates, such as classical plate theory (CPT), first-order shear deformation plate theory (FSDPT), and high-order shear deformation plate theory (HSDPT). There are many kinds of HSDPTs, such as HSDPT. Because the classical deformable plate theory does not consider shear deformation, only longitudinal wave and flexural wave are considered in the modeling process, and the influence of shear wave is ignored. Therefore, the evaluation of phase velocity and group velocity of flexural wave is much larger. The FSDPT considers longitudinal wave, shear wave and flexural wave, but shear factor needs to be considered in the modeling process. Although when selecting the size of shear factor, it needs to be treated carefully, but in general, it is more accurate and sufficient to use the FSDPT to model the plate theory. Therefore, in the establishment of our wave equation below, we use the FSDPT to derive the motion equations. Based on FSDPT, the component of displacement field in the FG nanoplate have the form (Sun and Luo 2011, Karami *et al*. 2018)

$$\begin{aligned} u &= z\varphi_x(x,y,t) + u_0(x,y,t) \\ v &= z\varphi_y(x,y,t) + v_0(x,y,t) \\ w &= w_0(x,y,t) \end{aligned} \tag{2}$$

Here, u_0, v_0 and w_0 are the midplane displacements of the FG nanoplate along the *x*, *y* and *z* direction, and φ_x and φ_y are the rotation along the *x* and *y* directions respectively, and *t* represents the time. From Eq. (2), we can see that FSDPT contains five degrees of freedom, However, CPT only contains three degrees of freedom. Compared with the three degrees of freedom problem, the establishment and solution of the dynamic equation of the five degrees of freedom problem will become more difficult.

According to the geometric equation, the strain component are (Sun and Luo 2011)

$$\begin{aligned} &\varepsilon_x = z\frac{\partial \varphi_x}{\partial x} + \frac{\partial u_0}{\partial x},\ \varepsilon_y = z\frac{\partial \varphi_y}{\partial y} + \frac{\partial v_0}{\partial y}, \\ &\varepsilon_{xy} = z\left(\frac{\partial \varphi_x}{\partial y} + \frac{\partial \varphi_y}{\partial x}\right) + \frac{\partial u_0}{\partial y} + \frac{\partial v_0}{\partial x}, \\ &\varepsilon_{xz} = \frac{\partial w_0}{\partial x} + \varphi_x,\ \varepsilon_{yz} = \frac{\partial w_0}{\partial y} + \varphi_y \end{aligned} \tag{3}$$

Here, ε_x represents the normal strain along the *x* direction, ε_y is the normal strain along the *y* direction, ε_{xy} stands for the shear strain in the *xy* plane, ε_{xz} refers to the shear strain in the *xz* plane, ε_{yz} is the shear strain in the *yz* plane.

The stress-strain relationship corresponding to NSG theory have the form

$$\Gamma_1\begin{Bmatrix}\sigma_x\\ \sigma_y\\ \sigma_{xy}\\ \sigma_{xz}\\ \sigma_{yz}\end{Bmatrix}=\Gamma_2\begin{bmatrix}S_{11} & S_{12} & 0 & 0 & 0\\ S_{12} & S_{22} & 0 & 0 & 0\\ 0 & 0 & S_{66} & 0 & 0\\ 0 & 0 & 0 & S_{44} & 0\\ 0 & 0 & 0 & 0 & S_{55}\end{bmatrix}\begin{Bmatrix}\varepsilon_x\\ \varepsilon_y\\ \varepsilon_{xy}\\ \varepsilon_{xz}\\ \varepsilon_{yz}\end{Bmatrix} \tag{4}$$

in which

$$\begin{aligned}&\Gamma_1=(1-l^2\nabla^2),\ \Gamma_2=[1-(ea)^2\nabla^2],\\ &S_{11}=S_{12}=\frac{E(z)}{1-\nu^2},\qquad S_{12}=\frac{\nu E(z)}{1-\nu^2},\\ &S_{66}=\frac{E(z)}{2(1-\nu)},\qquad S_{44}=S_{55}=\gamma^2 S_{66}.\end{aligned} \tag{5}$$

Here, we need to explain that *l* is a nanoscale parameter used to describe stiffness hardening (stain gradient parameter), and *ea* is a nanoscale parameter used to describe stiffness softening (nonlocal parameter), ∇ is the Laplacian operator. If we ignore the nano effect *ea* and *l*, which corresponds to the classical Newton theory. When *ea*=0, it corresponds to the strain gradient theory. When *l*=0, it corresponds to the nonlocal theory. In addition, we can also see that when *ea*=*l*, it also corresponds to the classical Newtonian mechanics theory. Many scholars have conducted extensive research on the application of NSG theory. Without considering the external force, by using the Hamilton principle, the motion equations can be derived as

$$\begin{aligned}&\Gamma_1\left(\frac{\partial N_x}{\partial x}+\frac{\partial N_{xy}}{\partial y}\right)=\Gamma_2\left(I_0\frac{\partial^2 u_0}{\partial t^2}+I_1\frac{\partial^2\varphi_x}{\partial t^2}\right)\\ &\Gamma_1\left(\frac{\partial N_y}{\partial y}+\frac{\partial N_{xy}}{\partial x}\right)=\Gamma_2\left(I_0\frac{\partial^2 v_0}{\partial t^2}+I_1\frac{\partial^2\varphi_y}{\partial t^2}\right)\\ &\Gamma_1\left(\frac{\partial Q_x}{\partial x}+\frac{\partial Q_y}{\partial y}\right)=\Gamma_2\left(I_0\frac{\partial^2 w_0}{\partial t^2}\right)\\ &\Gamma_1\left(\frac{\partial M_x}{\partial x}+\frac{\partial M_{xy}}{\partial y}-Q_x\right)=\Gamma_2\left(I_1\frac{\partial^2 u_0}{\partial t^2}+I_2\frac{\partial^2\varphi_x}{\partial t^2}\right)\\ &\Gamma_1\left(\frac{\partial M_y}{\partial y}+\frac{\partial M_{xy}}{\partial x}-Q_y\right)=\Gamma_2\left(I_1\frac{\partial^2 v_0}{\partial t^2}+I_2\frac{\partial^2\varphi_y}{\partial t^2}\right)\end{aligned} \tag{6}$$

in which, A_{ij}, B_{ij} and D_{ij} are the stiffness, coupling stiffness and bending stiffness of the NSG nanoplate, and

$$\begin{aligned}&\left(A_{ij},B_{ij},D_{ij}\right)=\int_{-\frac{h}{2}}^{\frac{h}{2}}S_{ij}(1,z,z^2)\ dz,\quad (i,j=1,2,6)\\ &A_{44}=A_{55}=\int_{-\frac{h}{2}}^{\frac{h}{2}}\gamma^2 S_{66}\ dz\\ &(I_0,I_1,I_2)=\int_{-\frac{h}{2}}^{\frac{h}{2}}\rho(z)(1,z,z^2)\ dz\end{aligned} \tag{7}$$

Substituting the constitutive equation into the above equation leads to the following equations of motion,

$$\begin{aligned}&(1-l^2\nabla^2)\left(A_{11}\frac{\partial^2 u_0}{\partial x^2}+A_{12}\frac{\partial^2 v_0}{\partial x\partial y}+B_{11}\frac{\partial^2\varphi_x}{\partial x^2}+B_{12}\frac{\partial^2\varphi_y}{\partial x\partial y}\right.\\ &\left.+A_{66}\left(\frac{\partial^2 u_0}{\partial y^2}+\frac{\partial^2 v_0}{\partial x\partial y}\right)+B_{66}\left(\frac{\partial^2\varphi_x}{\partial y^2}+\frac{\partial^2\varphi_y}{\partial x\partial y}\right)\right)\\ &=[1-(ea)^2\nabla^2]\left(I_0\frac{\partial^2 u_0}{\partial t^2}+I_1\frac{\partial^2\varphi_x}{\partial t^2}\right)\end{aligned} \tag{8}$$

$$\begin{aligned}&(1-l^2\nabla^2)\left\{A_{12}\frac{\partial^2 u_0}{\partial x\partial y}+A_{22}\frac{\partial^2 v_0}{\partial y^2}+B_{12}\frac{\partial^2\varphi_x}{\partial x\partial y}+B_{22}\frac{\partial^2\varphi_y}{\partial y^2}\right.\\ &\left.+A_{66}\left(\frac{\partial^2 u_0}{\partial x\partial y}+\frac{\partial^2 v_0}{\partial x^2}\right)+B_{66}\left(\frac{\partial^2\varphi_x}{\partial x\partial y}+\frac{\partial^2\varphi_y}{\partial x^2}\right)\right\}\\ &=[1-(ea)^2\nabla^2]\left(I_0\frac{\partial^2 v_0}{\partial t^2}+I_1\frac{\partial^2\varphi_y}{\partial t^2}\right)\end{aligned} \tag{9}$$

$$\begin{aligned}&(1-l^2\nabla^2)\left\{A_{44}\left(\frac{\partial\varphi_x}{\partial x}+\frac{\partial^2 w_0}{\partial x^2}\right)+A_{55}\left(\frac{\partial\varphi_y}{\partial y}+\frac{\partial^2 w_0}{\partial y^2}\right)\right\}\\ &=[1-(ea)^2\nabla^2]\left(I_0\frac{\partial^2 w_0}{\partial t^2}\right)\end{aligned} \tag{10}$$

$$\begin{aligned}&(1-l^2\nabla^2)\left\{B_{11}\frac{\partial^2 u_0}{\partial x^2}+B_{12}\frac{\partial^2 v_0}{\partial x\partial y}+D_{11}\frac{\partial^2\varphi_x}{\partial x^2}+D_{12}\frac{\partial^2\varphi_y}{\partial x\partial y}\right.\\ &\left.+B_{66}\left(\frac{\partial^2 u_0}{\partial y^2}+\frac{\partial^2 v_0}{\partial x\partial y}\right)+D_{66}\left(\frac{\partial^2\varphi_x}{\partial y^2}+\frac{\partial^2\varphi_y}{\partial x\partial y}\right)-A_{44}\left(\varphi_x+\frac{\partial w_0}{\partial x}\right)\right\}\\ &=[1-(ea)^2\nabla^2]\left(I_1\frac{\partial^2 u_0}{\partial t^2}+I_2\frac{\partial^2\varphi_x}{\partial t^2}\right)\end{aligned} \tag{11}$$

$$\begin{aligned}&(1-l^2\nabla^2)\left\{B_{12}\frac{\partial^2 u_0}{\partial x\partial y}+B_{22}\frac{\partial^2 v_0}{\partial y^2}+D_{12}\frac{\partial^2\varphi_x}{\partial x\partial y}+D_{22}\frac{\partial^2\varphi_y}{\partial y^2}\right.\\ &+B_{66}\left(\frac{\partial^2 u_0}{\partial x\partial y}+\frac{\partial^2 v_0}{\partial x^2}\right)+D_{66}\left(\frac{\partial^2\varphi_x}{\partial x\partial y}+\frac{\partial^2\varphi_y}{\partial x^2}\right)-A_{55}\left(\varphi_y\right.\\ &\left.\left.+\frac{\partial w_0}{\partial y}\right)\right\}\\ &=[1-(ea)^2\nabla^2]\left(I_1\frac{\partial^2 v_0}{\partial t^2}+I_2\frac{\partial^2\varphi_y}{\partial t^2}\right)\end{aligned} \tag{12}$$

From Eqs. (8) to (12), we can see that the wave equation contains five degrees of freedom. If *ea* and *l* are not considered at this time, the governing equation becomes

$$\begin{aligned}&\left(A_{11}\frac{\partial^2 u_0}{\partial x^2}+A_{12}\frac{\partial^2 v_0}{\partial x\partial y}+B_{11}\frac{\partial^2\varphi_x}{\partial x^2}+B_{12}\frac{\partial^2\varphi_y}{\partial x\partial y}\right.\\ &\left.+A_{66}\left(\frac{\partial^2 u_0}{\partial y^2}+\frac{\partial^2 v_0}{\partial x\partial y}\right)+B_{66}\left(\frac{\partial^2\varphi_x}{\partial y^2}+\frac{\partial^2\varphi_y}{\partial x\partial y}\right)\right)\\ &=\left(I_0\frac{\partial^2 u_0}{\partial t^2}+I_1\frac{\partial^2\varphi_x}{\partial t^2}\right),\\ &\left\{A_{12}\frac{\partial^2 u_0}{\partial x\partial y}+A_{22}\frac{\partial^2 v_0}{\partial y^2}+B_{12}\frac{\partial^2\varphi_x}{\partial x\partial y}+B_{22}\frac{\partial^2\varphi_y}{\partial y^2}\right.\\ &\left.+A_{66}\left(\frac{\partial^2 u_0}{\partial x\partial y}+\frac{\partial^2 v_0}{\partial x^2}\right)+B_{66}\left(\frac{\partial^2\varphi_x}{\partial x\partial y}+\frac{\partial^2\varphi_y}{\partial x^2}\right)\right\}\\ &=\left(I_0\frac{\partial^2 v_0}{\partial t^2}+I_1\frac{\partial^2\varphi_y}{\partial t^2}\right),\\ &\left\{A_{44}\left(\frac{\partial\varphi_x}{\partial x}+\frac{\partial^2 w_0}{\partial x^2}\right)+A_{55}\left(\frac{\partial\varphi_y}{\partial y}+\frac{\partial^2 w_0}{\partial y^2}\right)\right\}=\left(I_0\frac{\partial^2 w_0}{\partial t^2}\right),\\ &\left\{B_{11}\frac{\partial^2 u_0}{\partial x^2}+B_{12}\frac{\partial^2 v_0}{\partial x\partial y}+D_{11}\frac{\partial^2\varphi_x}{\partial x^2}+D_{12}\frac{\partial^2\varphi_y}{\partial x\partial y}\right.\\ &+B_{66}\left(\frac{\partial^2 u_0}{\partial y^2}+\frac{\partial^2 v_0}{\partial x\partial y}\right)+D_{66}\left(\frac{\partial^2\varphi_x}{\partial y^2}+\frac{\partial^2\varphi_y}{\partial x\partial y}\right)-A_{44}\left(\varphi_x\right.\\ &\left.\left.+\frac{\partial w_0}{\partial x}\right)\right\}=\left(I_1\frac{\partial^2 u_0}{\partial t^2}+I_2\frac{\partial^2\varphi_x}{\partial t^2}\right),\end{aligned} \tag{13}$$

$$\left\{B_{12}\frac{\partial^2 u_0}{\partial x\partial y}+B_{22}\frac{\partial^2 v_0}{\partial y^2}+D_{12}\frac{\partial^2 \varphi_x}{\partial x\partial y}+D_{22}\frac{\partial^2 \varphi_y}{\partial y^2}\right.$$
$$+B_{66}\left(\frac{\partial^2 u_0}{\partial x\partial y}+\frac{\partial^2 v_0}{\partial x^2}\right)+D_{66}\left(\frac{\partial^2 \varphi_x}{\partial x\partial y}+\frac{\partial^2 \varphi_y}{\partial x^2}\right)-A_{55}\left(\varphi_y\right.$$
$$\left.\left.+\frac{\partial w_0}{\partial y}\right)\right\}=\left(I_1\frac{\partial^2 v_0}{\partial t^2}+I_2\frac{\partial^2 \varphi_y}{\partial t^2}\right)$$

If the nonlocal parameter is not considered, but the strain gradient parameter is considered, the governing equation becomes

$$(1-l^2\nabla^2)\left(A_{11}\frac{\partial^2 u_0}{\partial x^2}+A_{12}\frac{\partial^2 v_0}{\partial x\partial y}+B_{11}\frac{\partial^2 \varphi_x}{\partial x^2}+B_{12}\frac{\partial^2 \varphi_y}{\partial x\partial y}\right.$$
$$\left.+A_{66}\left(\frac{\partial^2 u_0}{\partial y^2}+\frac{\partial^2 v_0}{\partial x\partial y}\right)+B_{66}\left(\frac{\partial^2 \varphi_x}{\partial y^2}+\frac{\partial^2 \varphi_y}{\partial x\partial y}\right)\right)$$
$$=\left(I_0\frac{\partial^2 u_0}{\partial t^2}+I_1\frac{\partial^2 \varphi_x}{\partial t^2}\right),$$
$$(1-l^2\nabla^2)\left\{A_{12}\frac{\partial^2 u_0}{\partial x\partial y}+A_{22}\frac{\partial^2 v_0}{\partial y^2}+B_{12}\frac{\partial^2 \varphi_x}{\partial x\partial y}+B_{22}\frac{\partial^2 \varphi_y}{\partial y^2}\right.$$
$$+A_{66}\left(\frac{\partial^2 u_0}{\partial x\partial y}+\frac{\partial^2 v_0}{\partial x^2}\right)+B_{66}\left(\frac{\partial^2 \varphi_x}{\partial x\partial y}\right.$$
$$\left.\left.+\frac{\partial^2 \varphi_y}{\partial x^2}\right)\right\}=\left(I_0\frac{\partial^2 v_0}{\partial t^2}+I_1\frac{\partial^2 \varphi_y}{\partial t^2}\right),$$
$$(1-l^2\nabla^2)\left\{A_{44}\left(\frac{\partial \varphi_x}{\partial x}+\frac{\partial^2 w_0}{\partial x^2}\right)+A_{55}\left(\frac{\partial \varphi_y}{\partial y}+\frac{\partial^2 w_0}{\partial y^2}\right)\right\}$$
$$=\left(I_0\frac{\partial^2 w_0}{\partial t^2}\right),$$
$$(1-l^2\nabla^2)\left\{B_{11}\frac{\partial^2 u_0}{\partial x^2}+B_{12}\frac{\partial^2 v_0}{\partial x\partial y}+D_{11}\frac{\partial^2 \varphi_x}{\partial x^2}+D_{12}\frac{\partial^2 \varphi_y}{\partial x\partial y}\right.$$
$$+B_{66}\left(\frac{\partial^2 u_0}{\partial y^2}+\frac{\partial^2 v_0}{\partial x\partial y}\right)+D_{66}\left(\frac{\partial^2 \varphi_x}{\partial y^2}+\frac{\partial^2 \varphi_y}{\partial x\partial y}\right)-A_{44}\left(\varphi_x\right.$$
$$\left.\left.+\frac{\partial w_0}{\partial x}\right)\right\}=\left(I_1\frac{\partial^2 u_0}{\partial t^2}+I_2\frac{\partial^2 \varphi_x}{\partial t^2}\right),$$
$$(1-l^2\nabla^2)\left\{B_{12}\frac{\partial^2 u_0}{\partial x\partial y}+B_{22}\frac{\partial^2 v_0}{\partial y^2}+D_{12}\frac{\partial^2 \varphi_x}{\partial x\partial y}+D_{22}\frac{\partial^2 \varphi_y}{\partial y^2}\right.$$
$$+B_{66}\left(\frac{\partial^2 u_0}{\partial x\partial y}+\frac{\partial^2 v_0}{\partial x^2}\right)+D_{66}\left(\frac{\partial^2 \varphi_x}{\partial x\partial y}+\frac{\partial^2 \varphi_y}{\partial x^2}\right)-A_{55}\left(\varphi_y\right.$$
$$\left.\left.+\frac{\partial w_0}{\partial y}\right)\right\}=\left(I_1\frac{\partial^2 v_0}{\partial t^2}+I_2\frac{\partial^2 \varphi_y}{\partial t^2}\right) \tag{14}$$

If the nonlocal parameter is considered, but the strain gradient parameter is not considered, the governing equation becomes

$$\left(A_{11}\frac{\partial^2 u_0}{\partial x^2}+A_{12}\frac{\partial^2 v_0}{\partial x\partial y}+B_{11}\frac{\partial^2 \varphi_x}{\partial x^2}+B_{12}\frac{\partial^2 \varphi_y}{\partial x\partial y}\right.$$
$$\left.+A_{66}\left(\frac{\partial^2 u_0}{\partial y^2}+\frac{\partial^2 v_0}{\partial x\partial y}\right)+B_{66}\left(\frac{\partial^2 \varphi_x}{\partial y^2}+\frac{\partial^2 \varphi_y}{\partial x\partial y}\right)\right)$$
$$=[1-(ea)^2\nabla^2]\left(I_0\frac{\partial^2 u_0}{\partial t^2}+I_1\frac{\partial^2 \varphi_x}{\partial t^2}\right),$$
$$\left\{A_{12}\frac{\partial^2 u_0}{\partial x\partial y}+A_{22}\frac{\partial^2 v_0}{\partial y^2}+B_{12}\frac{\partial^2 \varphi_x}{\partial x\partial y}+B_{22}\frac{\partial^2 \varphi_y}{\partial y^2}\right.$$
$$\left.+A_{66}\left(\frac{\partial^2 u_0}{\partial x\partial y}+\frac{\partial^2 v_0}{\partial x^2}\right)+B_{66}\left(\frac{\partial^2 \varphi_x}{\partial x\partial y}+\frac{\partial^2 \varphi_y}{\partial x^2}\right)\right\}$$
$$=[1-(ea)^2\nabla^2]\left(I_0\frac{\partial^2 v_0}{\partial t^2}+I_1\frac{\partial^2 \varphi_y}{\partial t^2}\right),$$
$$\left\{A_{44}\left(\frac{\partial \varphi_x}{\partial x}+\frac{\partial^2 w_0}{\partial x^2}\right)+A_{55}\left(\frac{\partial \varphi_y}{\partial y}+\frac{\partial^2 w_0}{\partial y^2}\right)\right\}$$
$$=[1-(ea)^2\nabla^2]\left(I_0\frac{\partial^2 w_0}{\partial t^2}\right),$$
$$\left\{B_{11}\frac{\partial^2 u_0}{\partial x^2}+B_{12}\frac{\partial^2 v_0}{\partial x\partial y}+D_{11}\frac{\partial^2 \varphi_x}{\partial x^2}+D_{12}\frac{\partial^2 \varphi_y}{\partial x\partial y}\right.$$
$$\left.+B_{66}\left(\frac{\partial^2 u_0}{\partial y^2}+\frac{\partial^2 v_0}{\partial x\partial y}\right)+D_{66}\left(\frac{\partial^2 \varphi_x}{\partial y^2}+\frac{\partial^2 \varphi_y}{\partial x\partial y}\right)-A_{44}\left(\varphi_x+\frac{\partial w_0}{\partial x}\right)\right\}$$
$$=[1-(ea)^2\nabla^2]\left(I_1\frac{\partial^2 u_0}{\partial t^2}+I_2\frac{\partial^2 \varphi_x}{\partial t^2}\right),$$
$$\left\{B_{12}\frac{\partial^2 u_0}{\partial x\partial y}+B_{22}\frac{\partial^2 v_0}{\partial y^2}+D_{12}\frac{\partial^2 \varphi_x}{\partial x\partial y}+D_{22}\frac{\partial^2 \varphi_y}{\partial y^2}\right.$$
$$\left.+B_{66}\left(\frac{\partial^2 u_0}{\partial x\partial y}+\frac{\partial^2 v_0}{\partial x^2}\right)+D_{66}\left(\frac{\partial^2 \varphi_x}{\partial x\partial y}+\frac{\partial^2 \varphi_y}{\partial x^2}\right)-A_{55}\left(\varphi_y+\frac{\partial w_0}{\partial y}\right)\right\}$$
$$=[1-(ea)^2\nabla^2]\left(I_1\frac{\partial^2 v_0}{\partial t^2}+I_2\frac{\partial^2 \varphi_y}{\partial t^2}\right) \tag{15}$$

Next, we will discuss these five different forms of waves.

3. Solution of wave equation

When the elastic wave propagates in an FG nanoplate with four edges clamped, the solution of Eq. (12) satisfying the four clamped boundary conditions can be set as (Sun and Luo 2011)

$$u_0(x,y,t)=\sum_{m,n=1,3,5\ldots}^{\infty}u_{mn}\,sin\left(\frac{m\pi}{a}x\right)sin\left(\frac{n\pi}{b}y\right)\mathbb{Q}$$
$$v_0(x,y,t)=\sum_{m,n=1,3,5\ldots}^{\infty}v_{mn}\,sin\left(\frac{m\pi}{a}x\right)sin\left(\frac{n\pi}{b}y\right)\mathbb{Q}$$
$$w_0(x,y,t)=\sum_{m,n=1,3,5\ldots}^{\infty}w_{mn}[1-cos\left(\frac{2m\pi}{a}x\right)][1$$
$$-cos\left(\frac{2n\pi}{b}y\right)]\mathbb{Q}$$
$$\varphi_x(x,y,t)=\sum_{m,n=1,3,5\ldots}^{\infty}\varphi_{mn}^{x}\,sin\left(\frac{2m\pi}{a}x\right)[1-cos\left(\frac{2n\pi}{b}y\right)]\mathbb{Q}$$
$$\varphi_y(x,y,t)=\sum_{m,n=1,3,5\ldots}^{\infty}\varphi_{mn}^{y}[1-cos\left(\frac{2m\pi}{a}x\right)]\,sin\left(\frac{2n\pi}{b}y\right)\mathbb{Q} \tag{16}$$

Here, $\mathbb{Q}$ is related to time quantity, wave number and other parameters, and has the following definition

$$\mathbb{Q}=\left(e^{i(\kappa_1 x+\kappa_2 y+\omega t)}+e^{i(\kappa_1 x+\kappa_2 y-\omega t)}\right) \tag{17}$$

It should be pointed out that, in Eqs. (16) and (17), u_{mn}, v_{mn}, w_{mn}, ϕ_{mn}^{x} and ϕ_{mn}^{y} are wave amplitude, κ_1 and κ_2 are wave numbers along the x and y direction, ω are circular frequency. By substituting Eqs. (16) and (17) into Eqs. (8)-(12), and by using Galerkin principle and orthogonality condition of mode function, after a series of operations. And in this paper, we only consider the first mode, that is m=n=1, and then, a function of eigenvalue can be obtained, that is

$$(\boldsymbol{K}-\omega^2\boldsymbol{M})[u_{11},v_{11},w_{11},\varphi_{11}^{x},\varphi_{11}^{y}]^T=0 \tag{18}$$

If the equation is to have a non-zero solution, it must have:

$$|\boldsymbol{K}-\omega^2\boldsymbol{M}|=0 \tag{19}$$

In Eq. (19), the stiffness matrix, mass matrix and displacement matrix are defined as follows

$$\boldsymbol{K}=\begin{bmatrix} k_{11} & k_{12} & k_{13} & k_{14} & k_{15} \\ k_{21} & k_{22} & k_{23} & k_{24} & k_{25} \\ k_{31} & k_{32} & k_{33} & k_{34} & k_{35} \\ k_{41} & k_{42} & k_{43} & k_{44} & k_{45} \\ k_{51} & k_{52} & k_{53} & k_{54} & k_{55} \end{bmatrix}$$
$$\boldsymbol{M}=(1+ea^2({\kappa_1}^2+{\kappa_2}^2))\begin{bmatrix} I_0 & 0 & 0 & 0 & 0 \\ 0 & I_0 & 0 & 0 & 0 \\ 0 & 0 & 9I_0 & 0 & 0 \\ 0 & 0 & 0 & 3I_2 & 0 \\ 0 & 0 & 0 & 0 & 3I_2 \end{bmatrix} \tag{20}$$

The elements appeared in the matrix are defined as follows

$$\begin{aligned}
k_{11}&=\left(1+l^2({\kappa_1}^2+{\kappa_2}^2)\right)A_{11}\left(\frac{\pi^2}{a^2}+\kappa_1^2\right)\\
&\quad+A_{66}\left(1+l^2({\kappa_1}^2+{\kappa_2}^2)\right)\left(\frac{\pi^2}{b^2}+\kappa_2^2\right)\\
k_{12}&=k_{21}=\left(1+l^2({\kappa_1}^2+{\kappa_2}^2)\right)(A_{12}+A_{66})\kappa_1\kappa_2\\
k_{14}&=-k_{41}=B_{11}\left(1+l^2({\kappa_1}^2+{\kappa_2}^2)\right)\frac{256i\kappa_1}{9\pi^2}\frac{\pi}{a}\\
k_{15}&=-k_{51}\\
&=(B_{12}+B_{66})(1+l^2({\kappa_1}^2+{\kappa_2}^2))\frac{128i\kappa_1}{9\pi^2}\frac{\pi}{b}\\
k_{22}&=(1+l^2({\kappa_1}^2+{\kappa_2}^2))A_{22}(\frac{\pi^2}{b^2}+\kappa_2^2)\\
&\quad+(1+l^2({\kappa_1}^2+{\kappa_2}^2))A_{66}(\frac{\pi^2}{a^2}+\kappa_1^2)\\
k_{24}&=-k_{42}=(B_{12}+B_{66})(1+l^2({\kappa_1}^2\\
&\quad+{\kappa_2}^2))\frac{128i\kappa_2}{9\pi^2}\frac{\pi}{a}\\
k_{25}&=-k_{52}=B_{22}(1+l^2({\kappa_1}^2+{\kappa_2}^2))\frac{256i\kappa_2}{9\pi^2}\frac{\pi}{b}\\
k_{33}&=9(1+l^2({\kappa_1}^2+{\kappa_2}^2))(A_{44}\kappa_1^2+A_{55}\kappa_2^2)\\
&\quad+12(1+l^2({\kappa_1}^2+{\kappa_2}^2))(A_{44}\frac{\pi^2}{a^2}+A_{55}\frac{\pi^2}{b^2})\\
k_{34}&=k_{43}=6(1+l^2({\kappa_1}^2+{\kappa_2}^2))A_{44}\frac{\pi}{a}\\
k_{44}&=3D_{11}(1+l^2({\kappa_1}^2+{\kappa_2}^2))(4\frac{\pi^2}{a^2}+\kappa_1^2)\\
&\quad+D_{66}(1+l^2({\kappa_1}^2+{\kappa_2}^2))(4\frac{\pi^2}{b^2}+3\kappa_2^2)\\
&\quad+3A_{44}(1+l^2({\kappa_1}^2+{\kappa_2}^2))\\
k_{45}&=k_{54}=4(D_{12}+D_{66})(1+l^2({\kappa_1}^2+{\kappa_2}^2))\frac{\pi^2}{ab}\\
k_{55}&=3D_{22}(1+l^2({\kappa_1}^2+{\kappa_2}^2))(4\frac{\pi^2}{b^2}+\kappa_2^2)\\
&\quad+D_{66}(1+l^2({\kappa_1}^2+{\kappa_2}^2))(4\frac{\pi^2}{a^2}+3\kappa_1^2)\\
&\quad+3A_{55}(1+l^2({\kappa_1}^2+{\kappa_2}^2))\\
k_{13}&=k_{23}=k_{31}=k_{32}=0\\
k_{35}&=k_{53}=6A_{55}(1+l^2({\kappa_1}^2+{\kappa_2}^2))\frac{\pi}{b}
\end{aligned} \tag{21}$$

We can see from Eq. (19) that the entire homogeneous linear equations have 5 unknowns ($u_{11}, v_{11}, w_{11}, \varphi_{11}^x, \varphi_{11}^y$), and the matrix of the coefficients of the homogeneous linear equations is also equal to 5. Therefore, the homogeneous linear equations have non-zero solutions. According to Kramer's law, if the coefficient determinant of homogeneous linear equations is not 0, the equations have a unique solution. From the dispersion Eq. (19), we can find five pairs of real solutions, which correspond to five different waves, the first two of which are expansion waves, that is u_{11}, v_{11}, the third wave corresponds to the bending wavew_{11}, and the fourth and fifth wave correspond to the shear wave $\varphi_{11}^x, \varphi_{11}^y$. Considering that the material has the same properties in the direction *x* and *y* directions, so we have $\kappa=\kappa_1=\kappa_2$, and the phase velocity C_p can be obtained by the expression $C_p=\frac{\omega}{\kappa}$,and the group can be obtained by $C_g=d\frac{\omega}{d\kappa}$.

4. Examples

In order to verify the correctness of this study, we consider the macro FG plates, that is, the size effect is neglected, *ea*=*l*=0, and there is no porosity in the FG plates. The physical parameters and geometrical dimensions of the materials are consistent with those in the literature, that is to say, *a*=*b*=20*h*=0.2 m, E_b=151 GPa, E_m=70 GPa, ρ_c=3000 kg/m^3, ρ_m=2707 kg/m^3, v_c=v_m=0.3.The phase velocities and group velocities of Sun and Luo (2011) are also shown in Figs. 2 and 3. By comparing with the existing results of Sun and Luo (2011), we find that our results (the dots) are in good agreement with their results (the lines), which verifies the correctness of this present study. In addition, we can also see that when the size effect is not considered, the phase velocity is a decreasing function of the wave number, and the group velocity is an increasing function of the wave number. However, when the wave number is large enough, the group velocity basically remains unchanged.

In the following studies, the physical parameters and geometrical dimensions of the material are: E_c=322.27 GPa, ρ_c=2307 Kg/m^3, υ_c=0.24 for Si_3N_4, E_m=207.79 GPa, ρ_m = 8166 Kg/m^3, υ_m=0.24 for SUS304. Moreover, only the expansion waves and the flexural waves will be discussed in the following research.

In Figs. 4 and 5, we respectively study the impacts of the size parameters (that is, the nonlocal parameters *ea* and the strain gradient parameters *l*) on the group velocity and phase velocity of the porous FG nanoplates. From the figure, we can see that when the wave number is very small, the size of the nonlocal parameters and the strain gradient parameters have little influence on the dispersion relationship. However, when the wave number is relatively large, the phase velocity and the group velocity have significant impact, which is consistent with the conclusion of the existing literature (Only when the values of nonlocal parameters and strain gradient parameters are large, the size parameters can affect the dispersion relationship). Moreover, nonlocal parameters represent the stiffness softening effect, and strain gradient parameters represent the stiffness strengthening effect. Specifically, when the size parameter is not considered, that is, at this time, *ea*=*l*=0, the phase velocity decreases sharply as the wave number rises, but when the wave number increases to a certain extent, the

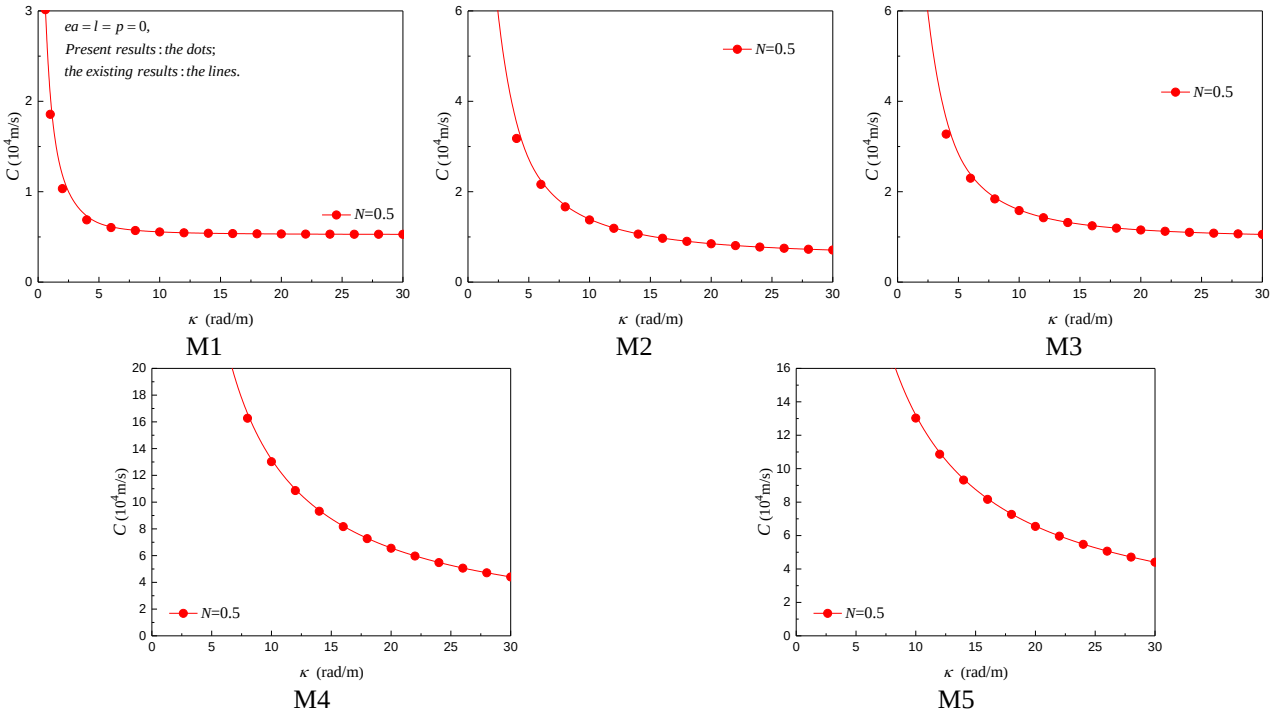

Fig. 2 Comparison of current phase velocities with phase velocities in Sun and Luo (2011)

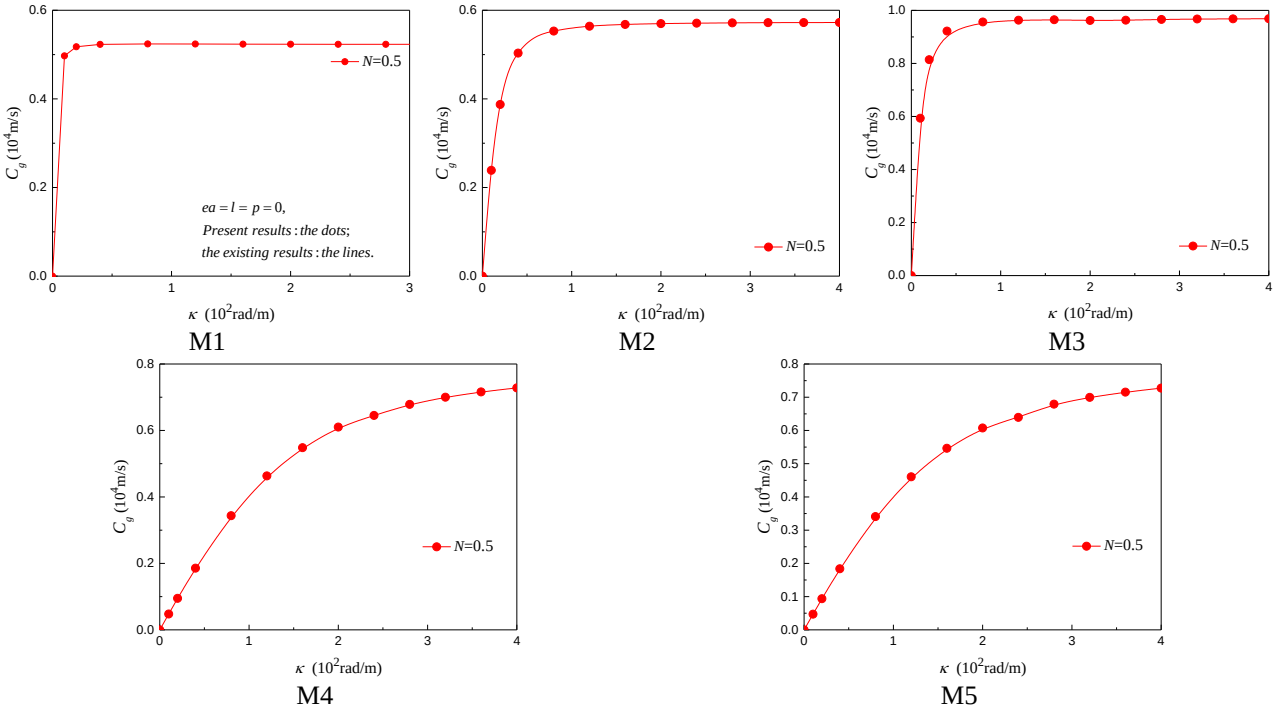

Fig. 3 Comparison of current group velocities with group velocities in Sun and Luo (2011)

phase velocity basically remains unchanged. However, when *ea*=0 and *l*=1 nm, the images at this time are obviously different. At the beginning, the phase velocity drops sharply with the increase of wave number. When the wave number increases to a certain value, the phase velocity basically remains unchanged, but when the wave number continues to increase, the phase velocity rises sharply. When *ea*=0 and *l*=2 nm, the phase velocity increases more significantly when the wave number is larger. That is to say, for *ea*=0, *l*=1 nm and *ea*=0, *l*=2 nm, when the wave number is small, the phase velocity is a decreasing function of the wave number; when the wave number is large, the phase velocity is an increasing function of the wave number. When *ea*=1 nm, *l*=0, the phase velocity is a subtractive function of the wave number. When *ea*=2 nm, *l*=0, the phase velocity is also a subtractive function of the wave

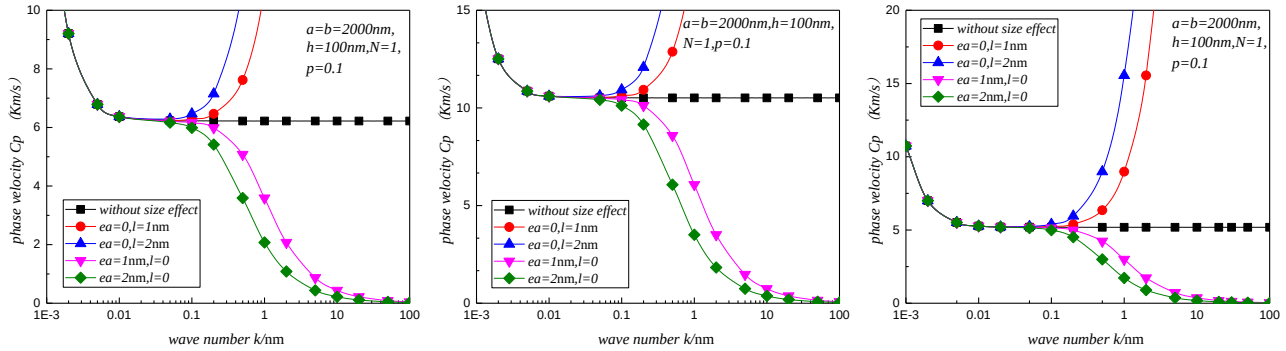

(a) The expansion wave u_{11} (b) The expansion wave v_{11} (c) The bending wave w_{11}

Fig. 4 Phase velocity diagrams for various *ea* and *l* at *a*=*b*=2000nm, *h*=100nm, *N*=1, *p*=0.1

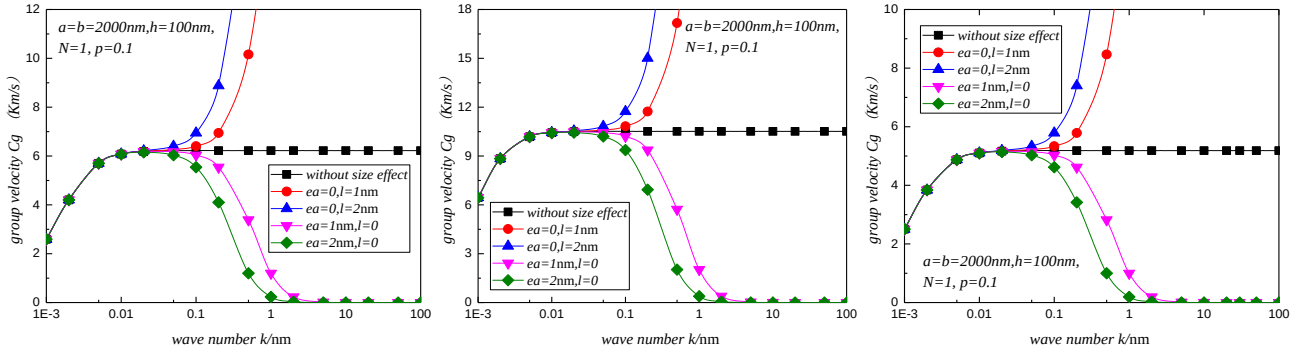

(a) The expansion wave u_{11} (b) The expansion wave v_{11} (c) The bending wave w_{11}

Fig. 5 Group velocity diagrams for various *ea* and *l* at *a*=*b*=2000nm, *h*=100nm, *N*=1, *p*=0.1

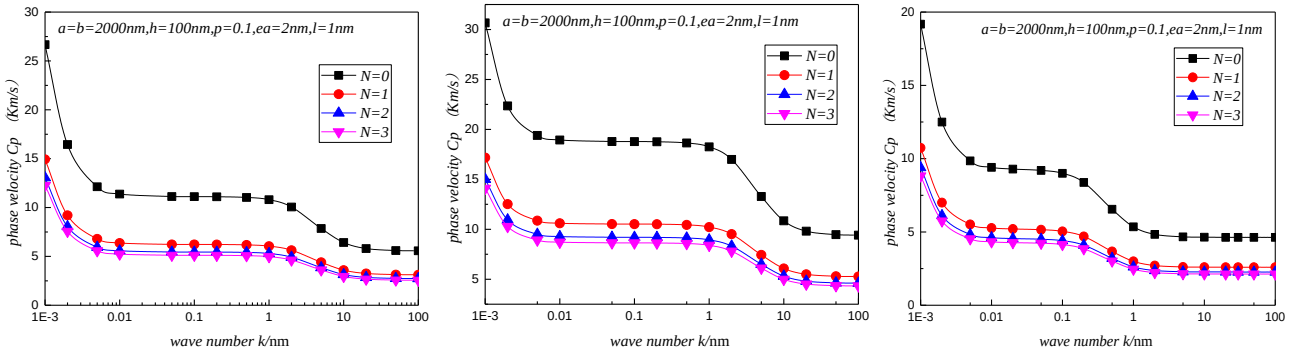

(a) The expansion wave u_{11} (b) The expansion wave v_{11} (c) The bending wave w_{11}

Fig. 6 Phase velocity diagrams for various *N* at *a*=*b*=2000nm, *h*=100nm, *ea*=2nm, *l*=1nm, *p*=0.1

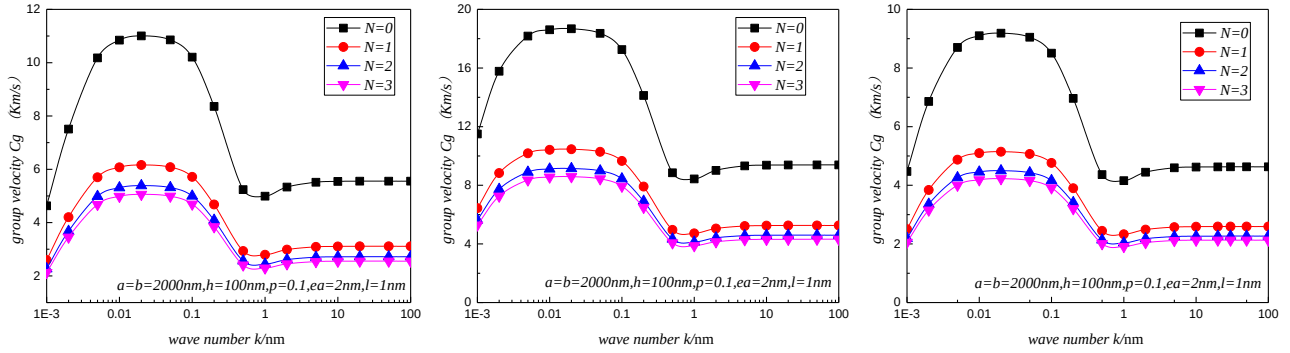

(a) The expansion wave u_{11} (b) The expansion wave v_{11} (c) The bending wave w_{11}

Fig. 7 Group velocity diagrams for various *N* at *a*=*b*=2000nm, *h*=100nm, *ea*=2nm, *l*=1nm, *p*=0.1

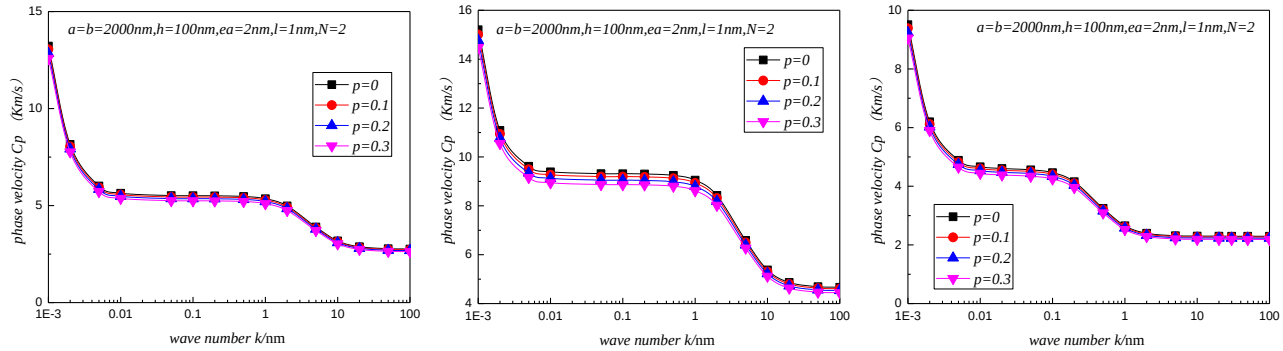

(a) The expansion wave u_{11} (b) The expansion wave v_{11} (c) The bending wave w_{11}

Fig. 8 Phase velocity diagrams for various p at a=b=2000nm, h=100nm, ea=2nm, l=1nm, N=2

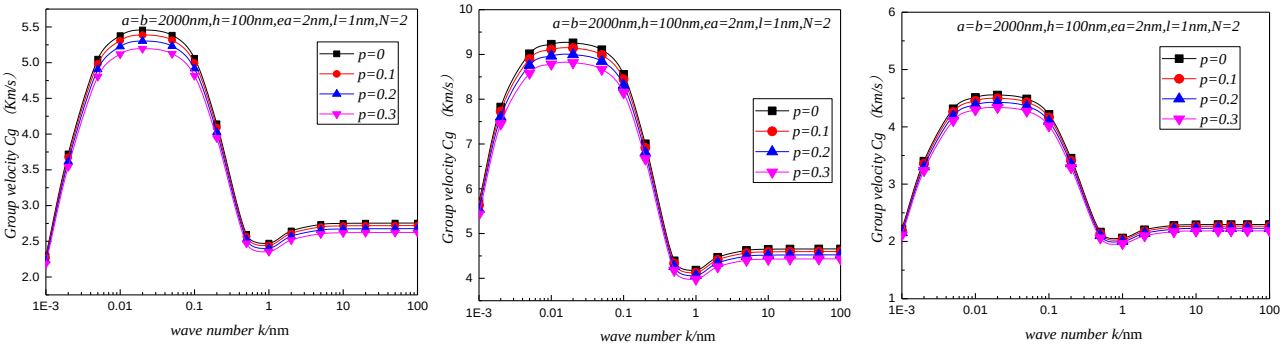

(a) The expansion wave u_{11} (b) The expansion wave v_{11} (c) The bending wave w_{11}

Fig. 9 Phase velocity diagrams for various p at a=b=2000nm, h=100nm, ea=2nm, l=1nm, N=2

number. In addition, we can also see that the change curve of group velocity and wave number is obviously different from the relationship curve of phase velocity and wave number. We can see from Fig. 5 that when the size effect is not considered, that is, when ea=l=0, the group velocity increases sharply at the beginning with the continuous increase of wave number, but when the wave number increases to a certain extent, the group velocity remains basically unchanged. When ea=0 and l=1 nm, and when ea=0 and l=2 nm, the group velocity initially increases sharply as the wave number goes up, but when the wave number increases to a certain extent, the group velocity basically remains unchanged, and when the wave number is still increasing, the group velocity increases sharply. When ea=1 and l=0 nm and when ea=2 nm and l=0 nm, the group velocity increases sharply with the continuous increase of the wave number. When the wave number increases to a certain extent, the group velocity decreases sharply, that is, the group velocity is the subtractive function of the wave number.

In Fig. 6 and Fig. 7, we respectively study the effect of the power law index parameter N on the group velocity and phase velocity. As seen, as N rises, the phase velocity and group velocity show a downward trend. It is obvious that with the decrease of the volume fraction of the ceramic, the elastic modulus and stiffness of the nano plate will decrease, which will lead to the decrease of the group velocity and phase velocity. Additionally, we can also find that under this condition, with the continuous increase of the wave number, the phase velocity is the subtraction function of the wave number, but the relationship curve between the group velocity and the wave number shows another phenomenon. At this time, with the continuous increase of the wave number, the group velocity first increases, then decreases, then increases again, and finally remains basically unchanged.

Similarly, with the increase of pore volume fraction p, the group velocity and phase velocity also decrease, See Figs. 8 and 9.

5. Conclusions

In this paper, we study the effects of nonlocal parameter, strain gradient parameter, porosity and power law index on wave propagation in porous NSG nanoplates. In the process of dynamic modeling, we use the first-order shear deformation plate theory. The first-order shear deformation theory contains two expansion waves, two shear waves and one bending wave. Then the dispersion relationship is obtained by using Galerkin principle. By solving the eigenvalue problem, the expressions of expansion wave, shear wave and bending wave are obtained. From the above analyses, we can know that: When the wave number is very small, the size of the nonlocal parameter and the strain gradient parameter have little influence on the dispersion relationship. On the contrary, when the wave number is relatively large, the phase velocity and the group velocity have significant impact. Nonlocal parameters represent the stiffness softening effect, and strain gradient parameters

represent the stiffness strengthening effect. With the decrease of the volume fraction of the ceramic, the elastic modulus and stiffness of the nano plate will decrease, which will lead to the decrease of the group velocity and phase velocity. The effect of pore is similar to that of power law index parameter, both of which have the effect of stiffness weakening, which results in the decrease of the group velocity and phase velocity.

References

Alazwari, M.A., Esen, I., Abdelrahman, A.A., Abdraboh, A.M. and Eltaher, M.A. (2022a), "Dynamic analysis of functionally graded (FG) nonlocal strain gradient nanobeams under thermo-magnetic fields and moving load", *Adv. Nano Res.*, **12**(3), 231-251. https://doi.org/10.12989/anr.2022.12.3.231.

Alazwari, M.A., Daikh, A.A. and Eltaher, M.A. (2022b), "Novel quasi 3D theory for mechanical responses of FG-CNTs reinforced composite nanoplates", *Adv. Nano Res.*, **12**(2), 117-137. https://doi.org/10.12989/anr.2022.12.2.117.

Akgöz, B. and Civalek, O. (2013), "A size-dependent shear deformation beam model based on the strain gradient elasticity theory", *Int. J. Eng. Sci.*, **70**, 1-14. https://doi.org/10.1016/j.ijengsci.2013.04.004.

Akgöz, B. and Civalek, O. (2014a), "Longitudinal vibration analysis for microbars based on strain gradient elasticity theory", *J. Vib. Control*, **20**(4), 606-616. https://doi.org/10.1177/1077546312463752.

Akgöz, B. and Civalek, O. (2014b), "Thermo-mechanical buckling behavior of functionally graded microbeams embedded in elastic medium", *Int. J. Eng. Sci.*, **85**, 90-104. https://doi.org/10.1016/j.ijengsci.2014.08.011.

Barretta, R. Ali Faghidian, S. and Marotti de Sciarra, F. (2019b), "Stress-driven nonlocal integral elasticity for axisymmetric nano-plates", *Int. J. Eng. Sci*., **136**, 38-52. https://doi.org/10.1016/j.ijengsci.2019.01.00.

Barretta, R., Sciarra, F.M.D. and Vaccaro, M.S. (2019a), "On nonlocal mechanics of curved elastic beams", *Int. J. Eng. Sci*., **144**, 103140. http://doi.org/10.1016/j.ijengsci.2019.103140.

Bouhadra, A., Menasria, A. and Rachedi, M.A. (2021), "Boundary conditions effect for buckling analysis of porous functionally graded nanobeam", *Adv. Nano Res.*, **10**(4), 313-325. http://doi.org/10.12989/anr.2021.10.4.313.

Civalek, O., Uzun,B., Yaylı, M.O., Akgöz, B. (2020), "Size-dependent transverse and longitudinal vibrations of embedded carbon and silica carbide nanotubes by nonlocal finite element method", *Eur. Phys. J. Plus*, **135**, 381. https://doi.org/10.1140/epjp/s13360-020-00385-w.

Ding, H.X. and She, G.L. (2021), "A higher-order beam model for the snap-buckling analysis of FG pipes conveying fluid", *Struct. Eng. Mech.*, **80**(1), 63-72. http://doi.org/10.12989/sem.2021.80.1.063.

Ebrahimi, F. and Barati, M. R. (2016), "Analytical solution for nonlocal buckling characteristics of higher-order inhomogeneous nanosize beams embedded in elastic medium", *Adv. Nano Res.*, **4**(3), 229-249. https://doi.org/10.12989/anr.2016.4.3.229.

Ebrahimi, F. and Barati, M. (2017), "A nonlocal strain gradient refined beam model for buckling analysis of size-dependent shear-deformable curved FG nanobeams", *Compos. Struct*., **159**(1), 174-182. http://doi.org/10.1016/j.compstruct.2016.09.058.

Ebrahimi, F., Barati, M.R. and Civalek, O. (2020), "Application of Chebyshev–Ritz method for static stability and vibration analysis of nonlocal microstructure-dependent nanostructures", *Eng. Comput.*, **36**, 953-964. https://doi.org/10.1007/s00366-019-00742-z.

Eltaher, M.A., Fouda, N., El-Midany, T. and Sadoun, A.M. (2018), "Modified porosity model in analysis of functionally graded porous nanobeams", *J. Brazil. Soc. Mech. Sci. Eng*., **40**(3), 141. https://doi.org/10.1007/s40430-018-1065-0.

Eltaher, M.A. and Abdelrahman, A.A. (2020), "Bending behavior of squared cutout nanobeams incorporating surface stress effects", *Steel Compos. Struct*., **36**, 143-161. http://doi.org/10.12989/scs.2020.36.2.143.

Fourn, H., Atmane, H.A., Bourada, M., Bousahla, A.A., Tounsi, A. and Mahmoud, S.R. (2018), "A novel four variable refined plate theory for wave propagation in functionally graded material plates", *Steel Compos. Struct*., **27**(1), 109-122. http://doi.org/10.12989/scs.2018.27.1.109.

Ghandourah, E.E., Ahmed, H.M., Eltaher, M.A., Attia, M.A., Abdraboh, A.M. (2021), "Free vibration of porous FG nonlocal modified couple nanobeams via a modified porosity model", *Adv. Nano Res.*, **11**(4), 405-422. http://doi.org/10.12989/anr.2021.11.4.405.

Jalaei, M.H. and Civalek, Ö. (2019), "On dynamic instability of magnetically embedded viscoelastic porous FG nanobeam", Int. *J. Eng. Sci*., **143**, 14-32. https://doi.org/10.1016/j.ijengsci.2019.06.013.

Karami, B., Janghorban, M. and Li, L. (2018), "On guided wave propagation in fully clamped porous functionally graded nanoplates", *Acta Astronaut*., **143**, 380-390. https://doi.org/10.1016/j.actaastro.2017.12.011.

Khadir, A.I., Daikh, A.A. and Eltaher, M. A. (2021), "Novel four-unknowns quasi 3D theory for bending, buckling and free vibration of functionally graded carbon nanotubes reinforced composite laminated nanoplates", *Adv. Nano Res.*, **11**(6), 621-640. https://doi.org/10.12989/anr.2021.11.6.621.

Lim, C.W., Zhang, G. and Reddy, J.N. (2015), "A higher-order nonlocal elasticity and strain gradient theory and its applications in wave propagation", *J. Mech. Phys. Solids*, **78**, 298-313. https://doi.org/10.1016/j.jmps.2015.02.001.

Liu, H. and Lv, Z. (2018), "Uncertain material properties on wave dispersion behaviors of smart magneto-electro-elastic nanobeams", *Compos. Struct*., **202**(15), 615-624. https://doi.org/10.1016/j.compstruct.2018.03.024.

Lu, L., She, G.L. and Guo, X. (2021), "Size-dependent postbuckling analysis of graphene reinforced composite microtubes with geometrical imperfection", *Int. J. Mech. Sci*., **199**, 106428. https://doi.org/10.1016/j.ijmecsci.2021.106428.

Ma, L.H., Ke, L.L., Reddy, J.N., Yang, J., Kitipornchai, S. and Wang, Y.S. (2018b), "Wave propagation characteristics in magneto-electro-elastic nanoshells using nonlocal strain gradient theory", *Compos. Struct*., **199**, 10-23. https://doi.org/10.1016/j.compstruct.2018.05.061.

Ma, L.H., Ke, L.L., Wang, Y.Z. and Wang, Y.S. (2017), "Wave propagation in magneto-electro-elastic nanobeams via two nonlocal beam models", *Physica E*, **86**, 253-161. https://doi.org/10.1016/j.physe.2016.10.036.

Ma, L.H., Ke, L.L., Wang, Y.Z. and Wang, Y.S. (2018a), "Wave propagation analysis of piezoelectric nanoplates based on the nonlocal theory", *Int. J. Struct. Stabil. Dyn.*, **18**(4), 1850060. https://doi.org/10.1142/S0219455418500608.

Malikan, M., Krasheninnikov, M., Eremeyev, V.A. (2020b), "Torsional stability capacity of a nano-composite shell based on a nonlocal strain gradient shell model under a three-dimensional magnetic field", *Int. J. Eng. Sci*., **148**, 103210. http://doi.org/10.1016/j.ijengsci.2019.103210.

Malikan, M., Uglov, N.S., Eremeyev, V.A. (2020a), "On instabilities and post-buckling of piezomagnetic and flexomagnetic nanostructures", *Int. J. Eng. Sci*., **157**, 103395. http://doi.org/10.1016/j.ijengsci.2020.103395.

Matouk, H., Bousahla, A.A., Heireche, H., Bourada, F., Bedia, E.A.A., Tounsi, A., Mahmoud, S.R., Tounsi, A. and Benrahou, K.H. (2020), "Investigation on hygro-thermal vibration of P-FG and symmetric S-FG nanobeam using integral Timoshenko beam theory", *Adv. Nano Res.*, **8**(4), 293-305. https://doi.org/10.12989/anr.2020.8.4.293.

Numanoğlu, H.M., Ersoy, H., Akgöz, B. and Civalek, O. (2022), "A new eigenvalue problem solver for thermo-mechanical vibration of Timoshenko nanobeams by an innovative nonlocal finite element method", *Math. Methods Appl. Sci.*, **45**(5), 2592-2614. https://doi.org/10.1002/mma.7942.

She, G.L., Liu, H.B. and Karami, B. (2021), "Resonance analysis of composite curved microbeams reinforced with graphene nanoplatelets", *Thin Wall. Struct*., **160**, 107407. https://doi.org/10.1016/j.tws.2020.107407.

She, G.L., Ding, H.X. and Zhang, Y.W. (2022), "Wave propagation in a FG circular plate via the physical neutral surface concept", *Struct. Eng. Mech.*, **82**(2), 225-232. http://doi.org/10.12989/sem.2022.82.2.225.

She, G.L. (2021), "Guided wave propagation of porous functionally graded plates: The effect of thermal loadings", *J. Therm. Stress.*, **44**(10), 1289-1305. https://doi.org/10.1080/01495739.2021.1974323.

Singh, P.P. and Azam, M.S. (2021), "Size dependent vibration of embedded functionally graded nanoplate in hygrothermal environment by Rayleigh-Ritz method", *Adv. Nano Res.*,**10**(1), 25-42. https://doi.org/10.12989/anr.2021.10.1.025.

Sun, D. and Luo, S.N., (2011), "The wave propagation and dynamic response of rectangular functionally graded material plates with completed clamped supports under impulse load", *Eur. J. Mech. A Solid*., **30**(3), 396-408. https://doi.org/10.1016/j.euromechsol.2011.01.001.

Wang, Y.Q. and Liang, C. (2019), "Wave propagation characteristics in nanoporous metal foam nanobeams", *Results Phys.*, **12**, 287-297. https://doi.org/10.1016/j.rinp.2018.11.080.

Wang, Y.Q., Liang, C. and Zu, J.W. (2019), "Wave propagation in functionally graded cylindrical nanoshells based on nonlocal Flügge shell theory", *Eur. Phys. J. Plus*, **134**(5), 233. https://doi.org/10.1140/epjp/i2019-12543-0.

Zemri, A., Houari, M.S.A., Bousahla, A.A. and Tounsi, A. (2015), "A mechanical response of functionally graded nanoscale beam: An assessment of a refined nonlocal shear deformation theory beam theory", *Struct. Eng. Mech.*, **54**(4), 693-710. https://doi.org/10.12989/sem.2015.54.4.693.

Zhang, Y.Y., Wang, Y.X., Zhang, X., Shen, H.M. and She, G.L., (2021), "On snap-buckling of FG-CNTR curved nanobeams considering surface effects", *Steel Compos. Struct*., **38**(3), 293-304. http://doi.org/10.12989/scs.2021.38.3.293.

Zhang, Y.W. and She, G.L. (2022), "Wave propagation and vibration of FG pipes conveying hot fluid", *Steel Compos. Struct*., **42**(3), 397-405. http://doi.org/10.12989/scs.2022.42.3.397.

Zhou, W.J., Chen, W.Q., Muhammad, Lim, C.W. (2019), "Surface effect on the propagation of flexural waves in periodic nano-beam and the size-dependent topological properties", *Compos. Struct.*, **216**, 427-435. https://doi.org/10.1016/j.compstruct.2019.03.016.